

# Confinement and gas fueling in LHD limiter discharges

K. Nishimura <sup>\*</sup>, K. Kawahata, K. Narihara, T. Morisaki, S. Masuzaki,  
S. Sakakibara, K. Tanaka, LHD Experimental Group

National Institute for Fusion Science, Oroshi-cho 322-6, Toki 509-5292, Japan

---

## Abstract

Plasma discharges in the Large Helical Device are normally open helical divertor discharges. To compare limiter discharges with open divertor discharges and to examine the role of the peripheral region, a radial movable limiter, whose head was made of carbon with high heat conductivity, was inserted into the plasma from the high field side (near the helical coil). The electron temperature was bounded well by the limiter. A high temperature gradient at the edge region was observed in both open divertor and limiter discharges. Formation of such a high temperature gradient led to good energy confinement even in the limiter discharges and an enhancement factor of  $1.1 \pm 0.3$  for International Stellarator Scaling 95 (ISS95) scaling was observed at every limiter position ( $0.75 < \rho < 1$ ). Serious degradation of the plasma confinement by increase of recycling and/or impurities was not observed in the limiter discharges. Within these experimental conditions, the dependence of the plasma minor radius on the energy confinement time was same as that of the ISS95 scaling law. A thick ergodic layer with  $R_{ax} = 3.75$  m prevents gas fueling by puffing.

© 2003 Elsevier Science B.V. All rights reserved.

PACS: 52.55

Keywords: Radially movable limiter; Energy confinement; Minor radius dependence; High edge temperature gradient; Fueling screening

---

## 1. Introduction

The Large Helical Device (LHD) [1–4] is the largest superconducting heliotron type device with  $l = 2/m = 10$  continuous helical coils and three pairs of poloidal coils. The major and minor radii of the plasma are 3.5–3.9 and 0.6–0.65 m, respectively. The maximum magnetic field strength is 2.89 T at the magnetic axis of  $R_{ax} = 3.6$  m. The achieved energy confinement time in LHD is systematically higher than that predicted by the International Stellarator Scaling 95 (ISS95) [5] by up to a factor of 1.6 and is comparable with ELM-*H*-mode confinement capability in tokamaks. This improvement in the overall energy confinement can be attributed to a reduction of electron thermal transport in the outer re-

gion of the plasma [6] resulting in a high temperature gradient at the edge region [7]. A radially movable limiter was inserted into the edge region in order to investigate the formation of high temperature gradient at the edge [8]. Formation of the high temperature gradient was observed at the edge region bounded by a limiter maintaining its width. No serious degradation of energy confinement was observed in the limiter experiment. The configuration with  $R_{ax} = 3.75$  m has a thicker ergodic layer than that of  $R_{ax} = 3.6$  m, and a such thick ergodic layer prevents gas fueling by puffing.

## 2. Experimental set-up

A radial movable limiter was installed at a lower port of LHD. Fig. 1 shows a schematic figure of the limiter and magnetic flux surfaces with  $R_{ax} = 3.6$  m. The limiter head, which is made of carbon (IG430U) with high thermal conductivity, is inserted into the plasma at the high field side (under the helical coil winding) as shown

<sup>\*</sup> Corresponding author. Tel.: +81-572 58 2169; fax: +81-572 58 2618.

E-mail address: [nishimura@lhd.nifs.ac.jp](mailto:nishimura@lhd.nifs.ac.jp) (K. Nishimura).

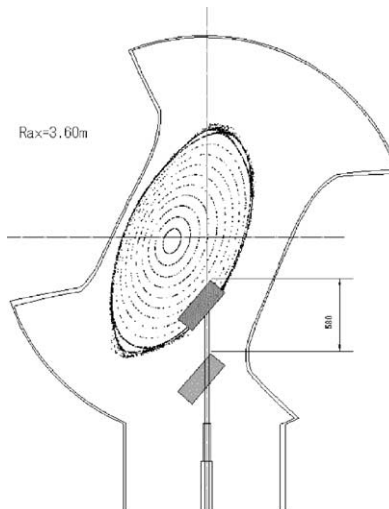


Fig. 1. Schematic figure of movable limiter.

in Fig. 1. The limiter size is  $420 \times 130 \times 30 \text{ mm}^3$ , and its position is controlled remotely with an accuracy of 0.5 mm. The objectives of the limiter experiments are as follows:

- (1) study of the dependence of the plasma minor radius on the energy confinement time,
- (2) comparison between open divertor discharges and limiter discharges on the formation of a high temperature gradient at the edge region,
- (3) study of the ergodic region surrounding the LHD core plasma.

### 3. Limiter function

Fig. 2 shows the comparison between calculated and measured divertor fluxes on the divertor plates in various limiter positions. Limiter position is expressed in flux coordinate normalized to the flux at the last closed flux surface, namely  $\rho = 1$  at the last closed flux surface. Divertor fluxes on the divertor plates were measured with the Langmuir probes installed on the divertor plates at various toroidal and poloidal positions. Calculated flux was deduced from the tracing the magnetic lines of force taking into account the random walk process [9], which simulates diffusive particle behavior, and the divertor plate where the field lines are terminated. The cross-field diffusion coefficient  $D$  is defined as  $D \sim C_s \rho^2 / \lambda$  where  $C_s$  is the sound speed,  $\rho$  the deviation length of a random walk and  $\lambda$  the step distance of the tracing. The diffusion coefficient  $D \sim 0.1 \text{ m}^2/\text{s}$  was used in this calculation. This value is the same order as that deduced from the density modulation experiment [10]. Although it is a small sized limiter, the divertor flux is obstructed well.

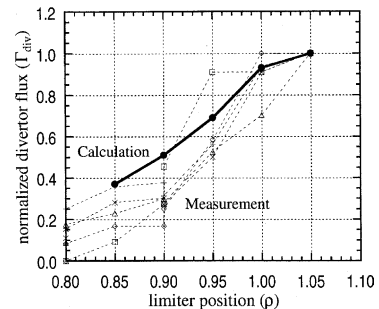


Fig. 2. Comparison of normalized divertor fluxes between calculation (solid line) and measurements (dashed lines). Data are normalized to the value at  $\rho = 1.05$ .

### 4. Formation of high temperature gradient at the edge region

Fig. 3 shows the electron temperature profiles measured with the multi-channel YAG Thomson scattering system [11] and the electron density profiles derived from a multi-channel FIR laser interferometer [12] measurement using Abel inversion. The arrows in this figure indicate the equivalent limiter position ( $\rho = 0.8$ ). The electron temperature profile was bounded well by the limiter but the plasma density profile was not bounded

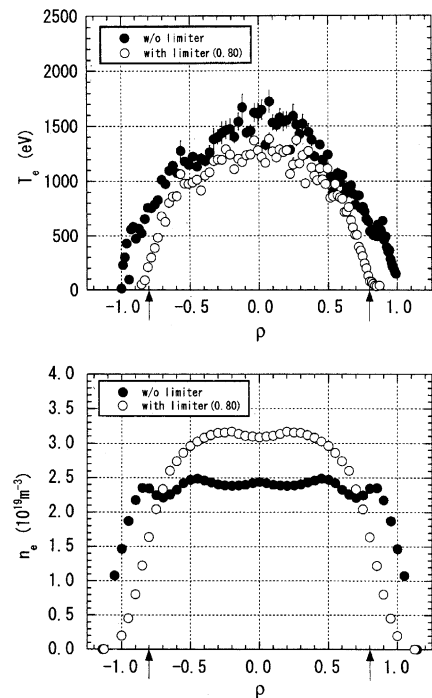


Fig. 3. Comparisons of electron temperature and density profiles with and without limiter. The equivalent limiter position is indicated by arrow.

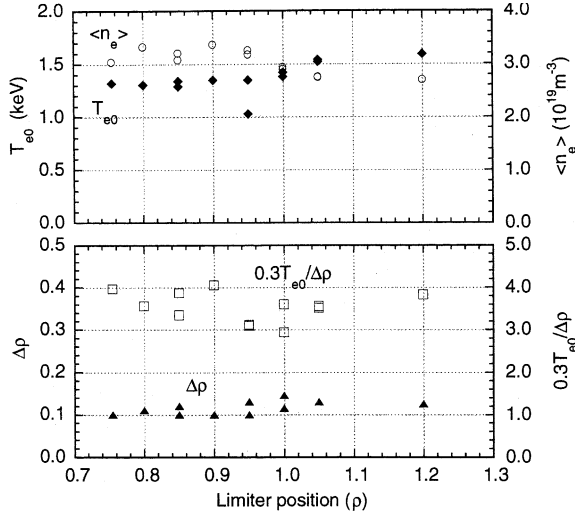


Fig. 4. Dependence of the plasma parameters on limiter position. The limiter position is expressed in normalized flux coordinate, and  $\rho = 1.2$  means the farthest position.

well. In the case of the open divertor discharge (without limiter), however, the plasma density exists in an ergodic region ( $\rho > 1.0$ ), which surrounds the closed magnetic surface region. A change of the electron temperature gradient can be seen at  $\rho \sim 0.85$  in the open divertor discharge and  $\rho \sim 0.6$  in the limiter discharge. Such high temperature gradient is also maintained in the limiter discharges.

Dependences of the central electron temperature ( $T_{e0}$ ), line averaged electron density ( $\langle n_e \rangle$ ), width of the edge region ( $\Delta\rho$ ), and the temperature gradient at the edge region ( $0.3T_{e0}/\Delta\rho$ ) on various limiter positions are shown in Fig. 4. The width of the edge region  $\Delta\rho$  was defined by the radius where the electron temperature is less than  $0.3T_{e0}$ , namely  $\Delta\rho = \rho(T_e = 0) - \rho(0.3T_{e0})$ . Linear fitting is used at the edge region. The position of  $\rho = 1.2$  in this figure means the farthest limiter position. The width of the edge region,  $\Delta\rho$ , are kept almost constant in every limiter position. As a result, a high temperature gradient at the edge region is also maintained in this experimental range.

## 5. Energy confinement characteristics

It was shown that the high temperature gradient at the edge region led to good energy confinement in divertor discharges [13] and such a configuration was similar to the internal thermal barrier in a tokamak [7]. Since the high temperature gradient at the edge region is observed in the limiter discharge, good energy confinement is also expected in the limiter discharges. Fig. 5 shows the normalized energy confinement time according

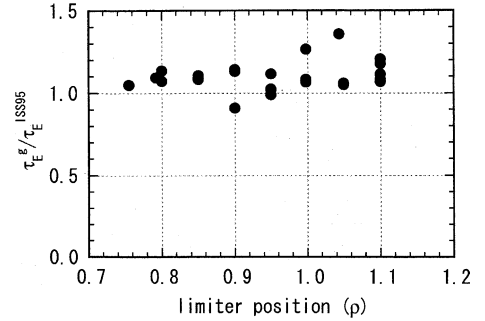


Fig. 5. Comparison of the energy confinement time with the ISS95 scaling.

to the ISS95 scaling at various limiter positions. The ISS95 scaling is expressed as follows [5]:

$$\tau_E^{\text{ISS95}} = 0.079 a_p^{2.21} R_p^{0.65} P_{\text{tot}}^{-0.59} \langle n_e \rangle^{0.51} B_t^{0.83} 2/3^{0.4},$$

where  $a_p$  and  $R_p$  are plasma minor and major radii in m, respectively, and  $P_{\text{tot}}$  is the total absorbed power in MW,  $\langle n_e \rangle$  is the line averaged electron density in  $10^{19} m^{-3}$ ,  $B_t$  is the magnetic field strength in Tesla, and  $2/3$  is the rotational transform at the radial position of  $2/3a_p$ . An enhancement factor of  $1.1 \pm 0.3$  over the predictions of the ISS95 scaling was observed at every limiter position. In this experiment, plasma parameters, except for  $a_p$ , were kept in same ranges and their dependences on  $\tau_E$  were weaker than that of  $a_p$ . According to this scaling, the change of  $a_p$  from 1.0 to 0.75 corresponds to a 44% change of  $\tau_E$ . Fig. 6 shows the dependence of the energy confinement time on the plasma minor radius. To exclude the contributions of the density and the absorbed power, the energy confinement time  $\tau_E^g$  is normalized by  $P_{\text{tot}}^{-0.59} \langle n_e \rangle^{0.51}$ . The solid line indicates the resulting curve of a regression analysis. This result agrees well with the ISS95 scaling within the error bar. So these results suggest the dependence of the energy confinement time on the plasma minor radius is in accordance with the ISS95 scaling.

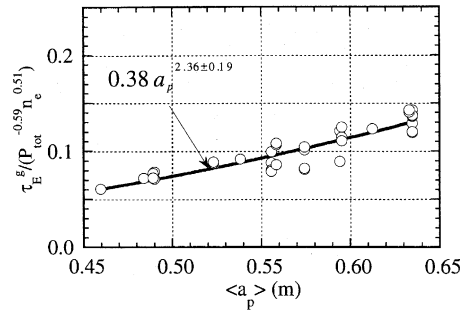


Fig. 6. Dependence of the energy confinement time on the plasma minor radius.

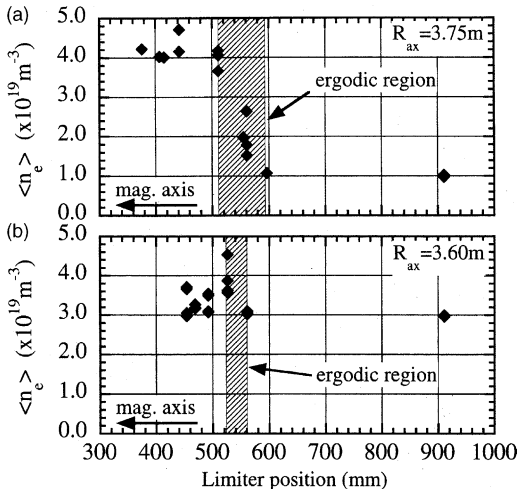


Fig. 7. Dependence of the line averaged electron densities on the limiter position in  $R_{ax} = 3.75\text{ m}$  and  $R_{ax} = 3.6\text{ m}$ .

## 6. Fueling characteristics

To investigate the role of the ergodic layer in gas fueling, the limiter is inserted into the ergodic region in  $R_{ax} = 3.75\text{ m}$  and  $R_{ax} = 3.6\text{ m}$  cases. Fig. 7 shows the dependences of the line averaged electron densities on the limiter position in  $R_{ax} = 3.75\text{ m}$  and  $R_{ax} = 3.6\text{ m}$ . Gas fueling is carried out with the gas puff system. The width of the ergodic layers are shown as hatched areas in Fig. 7. When the limiter is located just inside the plasma (limiter position 500 mm in Fig. 7), the line averaged electron densities are  $3\text{--}4 \times 10^{19} \text{ m}^{-3}$  both at  $R_{ax} = 3.75\text{ m}$  and  $R_{ax} = 3.6\text{ m}$  [14]. However, when the limiter position is far from the plasma (limiter position 910 mm in Fig. 7), the line averaged electron densities are  $1 \times 10^{19} \text{ m}^{-3}$  at  $R_{ax} = 3.75\text{ m}$  and  $3 \times 10^{19} \text{ m}^{-3}$  at  $R_{ax} = 3.6\text{ m}$ . This shows that the most of fueling gas in the case of  $R_{ax} = 3.75\text{ m}$  is ionized at the ergodic layer and does not reach the core region. In other words, the thickness of the ergodic layer in  $R_{ax} = 3.75\text{ m}$  is enough to ionize the most of fueling gas and that in  $R_{ax} = 3.6\text{ m}$  is not enough to ionize the most of fueling gas. With the insertion the limiter into the ergodic region, the width of the ergodic layer becomes smaller and the line averaged electron density becomes higher (Fig. 7(a)).

## 7. Summary

The radially movable limiter was inserted into the peripheral region of the LHD plasma. Although it is a

small sized limiter, the divertor flux is obstructed well. High temperature gradient at the edge region was observed both in open divertor and limiter discharges without serious degradation of the energy confinement time. This is circumstantial evidence that such high temperature gradient contributed to the high energy confinement. Dependence of the energy confinement time on the minor radius is in agreement with that of ISS95 scaling ( $a_p^{2.21}$ ). A thick ergodic layer prevents gas fueling by puffing.

## Acknowledgements

Authors would like to thank to the members of the device engineering group for their operational supports and former Director General A. Iiyoshi and Director General M. Fujiwara for their continuous encouragement.

## References

- [1] A. Iiyoshi, M. Fujiwara, O. Motojima, N. Ohyabu, K. Yamazaki, *Fus. Technol.* 17 (1990) 169.
- [2] O. Motojima, K. Akaishi, M. Asao, K. Fujii, et al., in: *Plasma Phys. and Contr. Nucl. Fus. Res. 1990 (Proc. 13th Int. Conf. Washington DC, 1990)*, vol. 3, IAEA, Vienna, 1990, p. 513.
- [3] A. Iiyoshi, A. Komori, A. Ejiri, M. Emoto, et al., *Nucl. Fusion* 39 (1999) 1245.
- [4] M. Fujiwara, H. Yamada, A. Ejiri, M. Emoto, et al., *Nucl. Fusion* 39 (1999) 1659.
- [5] U. Stroth, M. Murakami, R.A. Dory, H. Yamada, S. Okamura, F. Sano, T. Obiki, *Nucl. Fusion* 36 (1996) 1063.
- [6] H. Yamada, K.Y. Watanabe, S. Sakakibara, S. Murakami, et al., *Phys. Rev. Lett.* 84 (2000) 1216.
- [7] N. Ohyabu, K. Narihara, H. Funaba, T. Morisaki, et al., *Phys. Rev. Lett.* 84 (2002) 103.
- [8] K. Nishimura, H. Funaba, M. Goto, K. Ida, et al., *Proc. 12th Int. Stellarator Workshop*, Madison, 1999.
- [9] T. Morisaki, S. Masuzaki, M. Goto, S. Morita, A. Komori, et al., *Contrb. Plasma Phys.* 42 (2–4) (2002) 321.
- [10] K. Tanaka, K. Kawahata, T. Tokuzawa, H. Yamada, S. Murakami, et al., *J. Plasma Fusion Res. Series 4* (2001) 427.
- [11] K. Narihara, K. Yamauchi, I. Yamada, T. Minami, et al., *Fus. Eng. Des.* 34&35 (1997) 67.
- [12] K. Kawahata, K. Tanaka, Y. Ito, A. Ejiri, S. Okajima, *Rev. Sci. Instrum.* 17 (1993) 2220.
- [13] K. Ida, S. Kado, Y. Liang, *Rev. Sci. Instrum.* 71 (2000) 2360.
- [14] S. Morita, M. Goto, T. Morisaki, S. Masuzaki, S. Inagaki, et al., *Proc. 12th Int. Stellarator Workshop*, Madison, 1999.